Two- and Three-Dimensional Optical Tomography of Finger Joints for Diagnostics of Rheumatoid Arthritis

Alexander D. Klose[1], Andreas H. Hielscher[1], Kenneth M. Hanson[2] and Jürgen Beuthan[3]

[1] SUNY Health Science Center at Brooklyn, Dept. of Pathology, Brooklyn, NY 11203, USA
[2] Los Alamos National Laboratory, Hydrodynamic Applications, Los Alamos, NM 87545, USA
[3] FU Berlin, Institut für Medizinische Physik, 12207 Berlin, Germany

ABSTRACT

Rheumatoid arthritis (RA) is one of the most common diseases of human joints. This progressive disease is characterized by an inflammation process that originates in the inner membrane (synovalis) of the capsule and spreads to other parts of the joint. In early stages the synovalis thickness and the permeability of this membrane changes. This leads to changes in the optical parameters of the synovalis and the synovial fluid (synovia), which occupies the space between the bones. The synovia changes from a clear yellowish fluid to a turbid grayish substance. In this work we present two and three-dimensional reconstruction schemes for optical tomography of the finger joints. Our reconstruction algorithm is based on the diffusion approximation and employs adjoint differentiation techniques for the gradient calculation of the objective function with respect to the spatial distribution of optical properties. In this way, the spatial distribution of optical properties within the joints is reconstructed with high efficiency and precision. Volume information concerning the synovial space and the capsula are provided. Furthermore, it is shown that small changes of the scattering coefficients can be monitored. Therefore, optical tomography has the potential of becoming a useful tool for the early diagnosis and monitoring of disease progression in RA.

Keywords: optical tomography, image reconstruction, adjoint differentiation, rheumatoid arthritis

1. INTRODUCTION

In recent years, considerable research effort has been devoted to the development of techniques and methods for optical tomography (OT). The technology for making optical tomographic measurement on human subjects is nowadays readily available[1,2,3,4,5] and has been applied in a variety of pilot studies concerned with monitoring of blood oxygenation,[6,7,8,9,10,11,12,13] hemorrhage detection,[3,14,15,16] functional imaging of brain activities[17,18,19,20,21], Alzheimer diagnosis[22,23] and breast cancer detection.[2,24,25,26,27,28,29] Another possible application of OT is the investigation of human finger joints for early rheumatoid diagnostics and for monitoring the inflammation process.[30,31] The small dimensions involved, the diameter of a joint is approximately 1-2 cm, make this an ideal application for photon migration imaging.[32]

A major challenge remains the development of computer algorithms that transform these measurements into useful images of the interior of large organs. Other than x-rays, the near-infrared photons used in PMT do not cross the medium on a straight line from the source to the detector. Light is scattered and absorbed throughout the system. Hence, standard backprojection method have only limited success,[33,34] and other analytical reconstruction methods are only available for highly restrictive problems.[35,36,37,38,39] In general, either the optical properties of a reference medium have to be known, or/and it has to be assumed that the heterogeneities constitute only a small perturbation in a homogeneous background medium. In the special case of the finger joint, large differences in the scattering and absorption coefficients occur, which prohibits the use of perturbation-theory-based reconstruction schemes. Furthermore, these schemes are computationally very expensive since they require the inversion of large, full, ill-conditioned Jacobian matrices. To overcome the limitations of perturbation-based reconstruction algorithm, we have introduced in the past a non-perturbation, model-based iterative reconstruction (MOBIIR) schemes.[40,41]

In this work we extend our MOBIIR code to include 3D data. Before we will present details on the 3D-reconstruction scheme, we will first give some background information on rheumatoid arthritis of finger joints. We will show that the MOBIIR algorithm is capable of reconstructing optically highly inhomogeneous finger joints. Therefore, Optical Tomography has the potential to assist in the early diagnosis and monitoring of rheumatoid arthritis.

2. RHEUMATOID ARTHRITIS OF FINGER JOINTS

Rheumatoid Arthritis is an inflammation of human joints that most commonly occurs in joints of the hands and feet. It affects 1-2% of the world-population and approximately 2.1 million people in the US. It is a progressive disease, which currently can not be cured.[42]

The major components of a finger-joint system are the bones, cartilage, muscle, tendon, ligament, capsule and the synovial fluid. In a finger joint two bones are connected and are kept moveable around one axis. The bones belong to hard tissue and are covered with a protective cartilage layer within the joint. The capsule is a soft tissue and connects the bones of the finger and confines the joint. The ligament and the tendon are also a soft tissue and connect the two bones or the bone with the muscle, respectively. The joint cavity between the two finger bones has a size of approximately 200 microns and is filled with an almost none scattering liquid, called synovial fluid or synovia, which keeps the joint moveable and provides nutrition to the cartilage.

The rheumatoid inflammation process of these so-called proximal interphalangeal (PIP) joints is generally divided into four different stages. During the first stage of the inflammation process the inner lining of the capsule, also called synovialis, starts to swell and changes its permeability. Dissolved and detached cells of the capsule migrate into the synovial cavity. During the second stage parts of the capsule are growing into the synovial cavity. The cavity becomes physically smaller, and the synovia becomes more turbid. In the later stages, the rheumatoid inflammation process destroys the capsule entirely and starts to attack the bone.

Conventional imaging techniques like X-ray shadowgrams or computer tomography are only able to monitor hard tissues with a high sensitivity. They are not able to monitor the early inflammation process characterized by slight changes of the properties of the synovial fluid and the volume of the synovalis. Therefore, X-ray techniques are used for advanced rheumatoid stages with partly damaged bones in the region of the cavity.[43] Magnetic resonance imaging can be used to recover changes of soft-tissues when contrast agents are used.[44] But this method is currently still too expensive for long-term, routine monitoring of rheumatoid diseases. Ultra sonic imaging techniques only allow to recover boundary layers, where the refraction index of ultra sonic waves is changed. It is mainly used in large joints, such as the shoulder. Ultrasound fails to detect very early stages of the inflammation, when significant changes of the thickness of the capsule have not yet occurred.[45] A complete survey about the optical properties connected to the rheumatoid arthritis of finger joints can be found at Prapavat.[46]

Given the process of this inflammatory disease, information about the optical properties of the synovalis, obtained from optical tomography, could be used to distinguish between healthy and rheumatoid conditions. Additionally, the optical properties of the synovial fluid indicate the various stages of the inflammation process. Therefore, optical techniques could not only be used to detect early stages of rheumatoid arthritis but also to monitor the inflammation process during the administration of medication. The rheumatoid inflammation is not a steady state but rather an alternating process between highly inflammated and more or less relaxed conditions, which could be optically monitored. The optical properties of the tissues and fluids involved were recently measured by Prapavat et al and are summarized in Table 1.

	reduced scattering coeff. μ'_s in cm^{-1}	absorption coeff. μ_a in cm^{-1}
Synovial membrane (healthy)	5.0	0.15
Synovial membrane (rheumatoid)	12.0	0.24
Synovia fluid (healthy)	0.06	0.004
Synovial fluid (rheumatoid)	0.12	0.011

Table 1: Optical Properties of finger joint tissues for the healthy and the rheumatoid condition at λ = 685 nm. [47]

3. MODEL-BASED RECONTRUCTION METHOD

Our three-dimensional iterative image reconstruction scheme is a model-based reconstruction method. It does not require the mentioned assumptions and promises to get better reconstructions of highly heterogeneous media with large perturbers. It combines a fast forward algorithm based on a finite-difference formulation of the time-dependent diffusion equation with zero-boundary conditions, an image analysis scheme and sensitivity calculations. These three components work together as follows:

The forward simulations are used to predict the detector readings based on an initial guess of the spatial distribution of optical properties in the simulated finger joint (diffusion coefficient, $D = c[3\mu_a+3\mu_s']^{-1}$ and absorption coefficient, μ_a). In this work we employ a finite difference scheme, which uses centered-space differences and a forward-time difference. The obtained three-dimensional difference equation for each time step and grid point is broken up into

three time steps and is solved for each spatial direction separately by means of an Alternating Direction Implicit Method (ADI).[48] It yields with U as intensity, S as source term, Δt as time step and c as light speed:

$$(1+c\mu_a\frac{\Delta t}{3})U_{i,j,k}^{n+1/3}-\frac{\Delta t}{3}\delta_{x_1}(U_{i,j,k}^{n+1/3})=\frac{\Delta t}{3}\delta_{x_2}(U_{i,j,k}^{n})+\frac{\Delta t}{3}\delta_{x_3}(U_{i,j,k}^{n})+U_{i,j,k}^{n}+\frac{\Delta t}{6}(S_{i,j,k}^{n+1}+S_{i,j,k}^{n})$$

The centered-space discretization of the spatial derivatives is defined as:

$$\delta_{x_p}(U_{i,j,k})\equiv[D_{i+1/2,j,k}(U_{i+1,j,k}-U_{i,j,k})-D_{i-1/2,j,k}(U_{i,j,k}-U_{i-1,j,k})]/\Delta x_p^{\,2}.$$

This discretization of the diffusion equation for each grid point and time step yields a system of difference equations and can therefore also be described in matrix notation:

$$AU^{n+1}=(B+C)U^{n}+S^{n}$$

An appropriate ordering of the intensity vector U^n and U^{n+1} yields a tri-diagonal matrix A. The system is solved forward in time for all U^{n+1} and for all grid points using a fast inversion of the matrix A. The ADI scheme is unconditionally stable in two dimensions and conditionally stable in three dimensions.

The predictions of the forward calculation are compared to the measurements by defining an objective function Φ. The reconstruction process can be accelerated due to the known positions and optical parameters of different tissue parts in the initial guess. Also the known healthy condition of a finger joint can be used as an initial guess. The objective function is defined as:

$$\Phi(D,\mu_a)=\sum_{s\in M}1/2\sigma(s)^2\sum_{n}(Y_s^n-U_s^n(D,\mu_a))^2$$

with the measurement Y, predictions U at the detector positions s for all time steps n.

To iteratively minimize the objective function Φ we use the gradient of Φ with respect to the spatial distribution of D. For the gradient calculation we employ the technique of adjoint differentiation (AD). In contrast to other computationally intensive approaches, the gradient calculations with AD parallels the forward computation in complexity and can be accomplished in the same time as one forward calculation. We obtain the gradient with respect to the diffusion coefficient as: [40,41]

$$\frac{d\Phi}{dD_r}=\sum_{n\in T}\sum_{p\in\Omega}\frac{d\Phi}{dU_p^n}\frac{\partial U_p^n}{\partial D_r}$$

Based on the gradient calculation the spatial distribution of D is updated within a line-minimization scheme, which makes use of a conjugated-gradient method. [49] The next iteration step begins with a new forward calculation. The reconstruction is completed when a minimum of the objective function is reached within a specified accuracy. A more detailed description of the algorithm can be found elsewhere. [50]

4. RECONSTRUCTION RESULTS

The following results are all based on simulated time-resolved data. To obtain these simulated data, we assigned the diffusion and absorption coefficients to MRI cross-section images of a human PIP joint (see Fig.1a,b). Since not all tissue types are clearly distinguishable by MRI data alone, standard anatomical information[51] was additionally used to uniquely identify the various positions of different tissues. The optical properties of different tissue parts like capsule, synovial fluid or bone are known from the literature.[46] After segmenting the MRI images we got two-dimensional (2D) slices of the optical properties in a finger joint. These images had a size of 44 by 44 pixels with a step width of 0.4 mm. Three-dimensional (3D) maps were generated by combining these 2D slices. In order to simulate measurements of the finger joint, we placed 16 detectors and 16 sources around the joint and performed forward calculations that yielded detector readings for different source positions. Gaussian noise at a level of 30dB was added to the artificial measurements simulating real-wold measurement conditions.

We used the simulated detector readings to reconstruct two-dimensional and three-dimensional maps of a healthy finger joint. Figure 1c shows the result for a two-dimensional reconstruction of the slice shown in Fig. 1b. This image was obtained after 200 iterations, which took 190 minutes on a SGI-Challenge L workstation with two R4400 processors. The

initial guess was a homogeneous medium with D = 1.03 $cm^2\ ns^{-1}$ (μ_s' = 7.0 cm^{-1} and μ_a = 0.1 cm^{-1}). It can be seen that the positions of the bone, ligament and tendon are well reconstructed. Furthermore, the absolute values of the diffusion coefficients are reconstructed within 10% of the original, even though these values can not be considered small perturbation with respect to the homogeneous initial guess. This clearly demonstrates the advantages of this non-perturbation approach to the reconstruction problem.

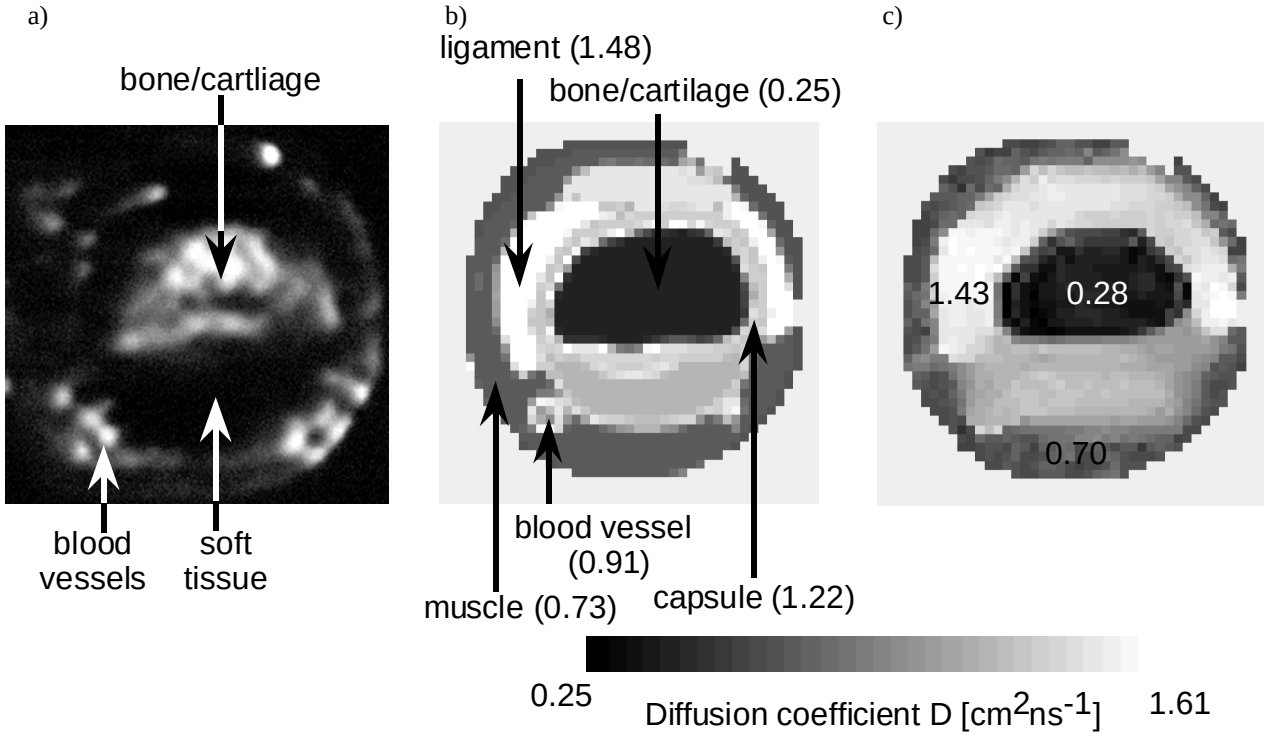

Fig. 1: a) original MRI image with the bone, muscle, tendon and ligament b) original map of the diffusion coefficients assigned to the MRI map c) reconstruction of diffusion coefficients after 200 iterations

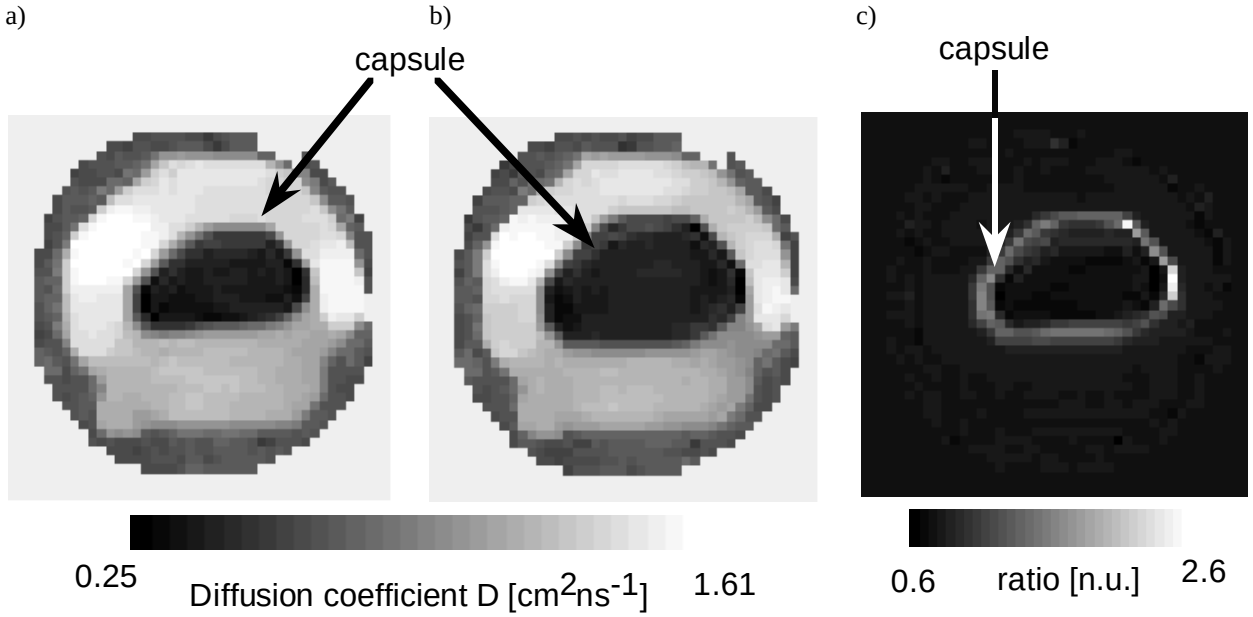

Fig.2: a) reconstruction of a healthy stage b) reconstruction of a rheumatoid stage c) ratio healthy/rheumatoid

As a second example, we investigated how changes in the optical properties of the capsule affect the reconstruction. The simulated capsule had a thickness of approximately 500-1000 microns, which corresponds to 1-3

pixels in our image. The reduced scattering coefficient in the healthy stage was $\mu_s' = 5$ cm^{-1}, while for the rheumatoid stage we chose $\mu_s' = 12$ cm^{-1}. The absorption coefficient, $\mu_a = 0.1$ cm^{-1}, was the same in both cases. After calculating the detector readings for both conditions, iterative reconstructions were performed starting with a homogeneous initial guess of $D = 1.03$ cm^2 ns^{-1} ($\mu_s' = 7.0$ cm^{-1} and $\mu_a = 0.1$ cm^{-1}). The results after 50 iterations (70 minutes) are shown in Fig. 2a,b. As can be seen differences between the simulated healthy and rheumatoid case only affect a small area occupied by the capsule. This becomes even clearer if we take the ratio of the two images (Fig. 2c). The ratio of both reconstructed images at the position of the capsule is 2.2 to 2.6, which is very close to the ratio of the original images with 2.4. In other areas the ratio is approximately 1.0±0.05. This demonstrates that the MOBIIR algorithm applied to finger joint systems has an excellent resolution and can successfully distinguish between small changes starting from a homogeneous initial guess far away from true distribution of optical properties.

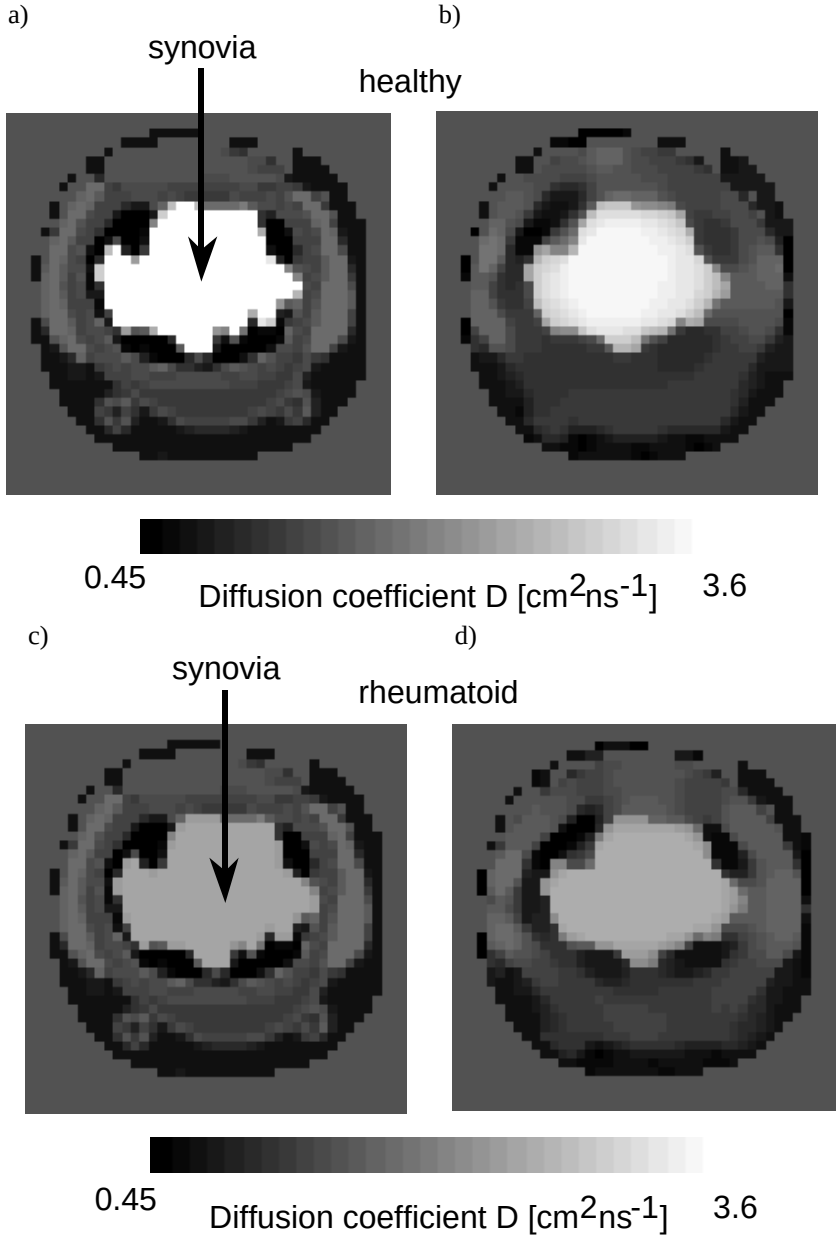

Fig. 3 Original images of the healthy (a) and the rheumatoid (c) stage and reconstructed images of the healthy (b) and rheumatoid (d) stage

Another way to detect the inflammation process is to reconstruct the diffusion coefficients of the synovial fluid in the cavity between the bones. The fluid occupies a space of only 200 μm between the two bones. Since the pixel size in

our three-dimensional maps is 800 μm, the optical properties had to be averaged in this area. We assumed a diffusion coefficient D=3.6 cm^2ns^{-1} for the synovial fluid in a healthy stage, and D=2.5 cm^2ns^{-1} for the fluid in a rheumatoid stage. Changes of the properties of the capsule were not considered. As an initial guess for the reconstruction we used anatomical information of a finger joint with D=3.0 cm^2ns^{-1} for the synovial fluid. An initial guess close to the real structure of the interior of a joint accelerates the reconstruction process and facilitates the convergence of the optimization to a local minimum of the objective function. However, as the earlier examples show is not a prerequisite in our reconstruction scheme. Figure 3 shows the reconstruction results after 60 iterations. It can be seen that the MOBIIR code can clearly distinguish between the healthy and rheumatoid stages.

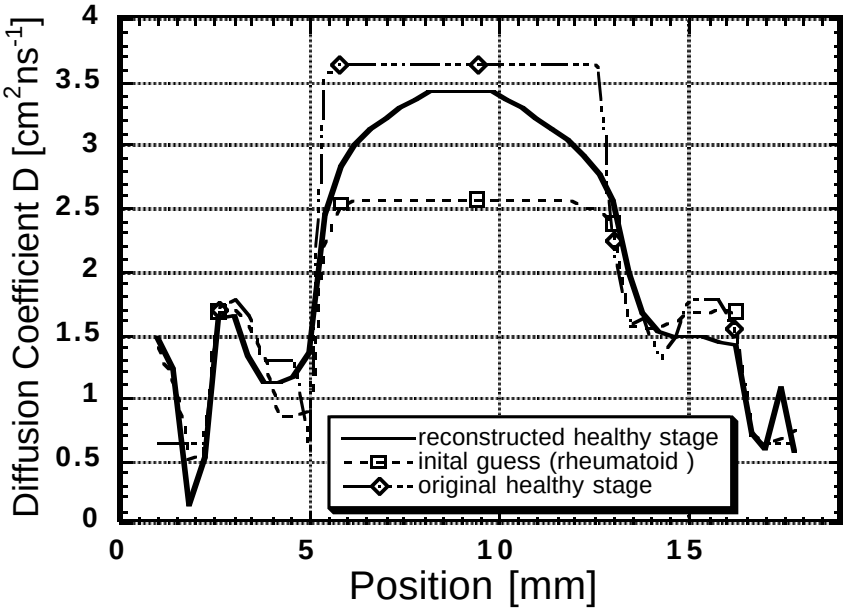

Fig.4 a) reconstructed healthy stage with a rheumatoid stage as initial guess

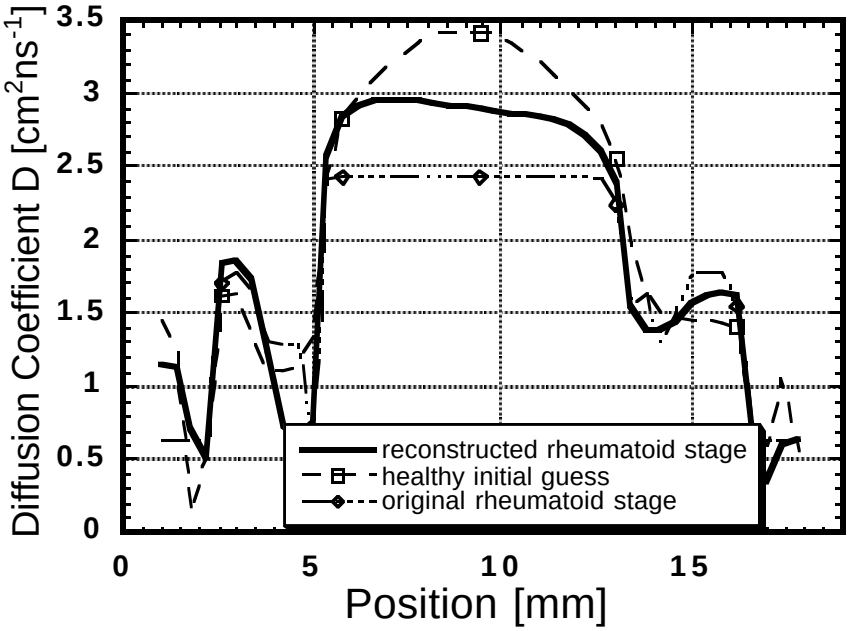

Fig 4.b) reconstructed rheumatoid stage with a healthy stage as initial guess

It is also interesting to monitor the changes of the synovia during the progression of the inflammation process. Therefore, we applied the following approach. We started with an initial guess of a healthy finger joint. In case of a rheumatoid inflammation of the PIP joint one gets a reconstructed image of a rheumatoid joint. Now we assume that after a certain time the inflammation decreases due to, for example, applying medication. Thus, we start another reconstruction with the rheumatoid stage from the previous calculation as an initial guess and assume the finger joint persists in a healthy condition. As a reconstruction we got the result as shown in Fig.4a. Fig.4a shows a cross section through the center of the synovial cavity of a finger joint. The joint has a diameter of 18 mm. In the middle one can clearly see the higher diffusion coefficients of the synovial fluid. Closer to the boundaries the diffusion coefficients become smaller because of the fat, ligament and capsule. The dashed line is the initial guess and denotes an inflammated joint. The dashed and dotted line means the healthy stage, which the joint is persisting in. The bold line is the calculated reconstruction that is based on the initial guess. It is also possible to do the opposite case. We assumed that the inflammation process proceeded again. Thus we took the former healthy joint as an initial guess and reconstructed the current rheumatoid condition. The result is shown in Fig.4b. In both images one can clearly see the distinct differences between both conditions.

In case of a synovial fluid with a very high diffusion coefficient the algorithm fails to reconstruct this part very well because of the large differences compared to the surrounded area of relatively low diffusion coefficients. This same result we observed for the three-dimensional reconstruction algorithm.

Finally, we also performed three-dimensional reconstructions. We added different MRI slices to get a three-dimensional model of a PIP joint in a healthy and rheumatoid stage. The three-dimensional model consisted of 9 slices with 30x30 pixel in each slice. The distances between the slices were 0.8 mm and the step size of each pixel was 0.8 mm too. Thus, the three-dimensional model consisted of 8100 voxels. The 8 detectors and 8 sources were located in 4 layers around the area of the capsule. In the healthy stage we assume $D=1.43\ cm^2ns^{-1}$ for the capsule, and $D=1.78\ cm^2ns^{-1}$ for the synovial fluid. For the rheumatoid stage we assumed $D=0.8\ cm^2ns^{-1}$ for the capsule and $D=0.9\ cm^2ns^{-1}$ for the fluid. For all other parts of the joints we chose optical properties as in Fig. 1b.

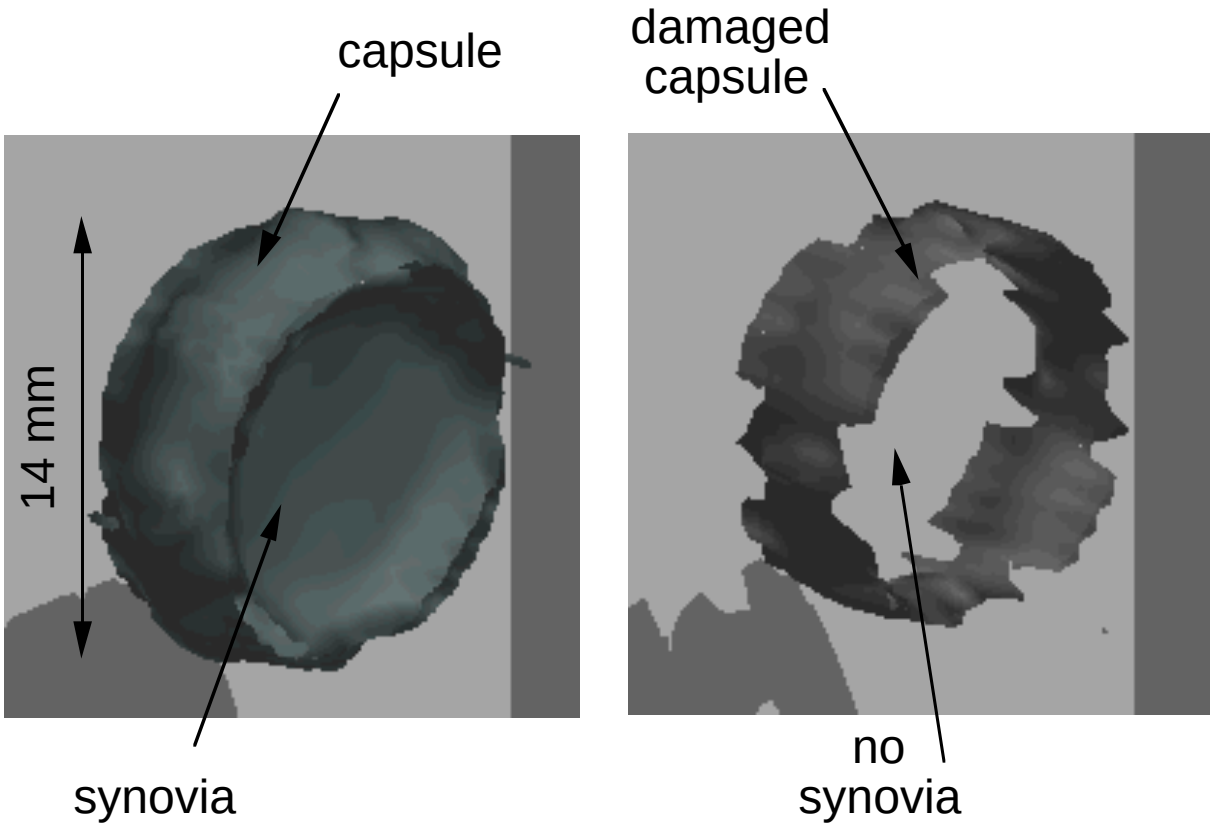

Fig. 5: 3D reconstruction of finger joint capsule model: (a) healthy condition, (b) rheumatoid condition. In the volume shown, D is larger than $0.78cm^2ns^{-1}$

The results of the reconstructions are shown in Fig. 5. Both reconstructions started with the same initial guess. The initial guess was a homogeneous media, which only contains the position of the bone and its diffusion coefficient. In

the shown figures the iso-surface with a constant diffusion coefficient of $0.78 cm^2 ns^{-1}$ are displayed for the healthy (Fig. 5a) and rheumatoid (Fig. 5b) stage. These surfaces confine a certain volume of the capsule and the synovial fluid. In case of a joint with RA the amount of voxels with a diffusion coefficient higher than a defined threshold is smaller than in the healthy one. Thus, a three-dimensional reconstruction scheme is able to recover a three-dimensional distribution of the diffusion coefficients of a joint. An iso-surface allows to determine a volume of a certain amount of voxel with a higher diffuison coefficient than the iso-surface.

We used only the position of hard and soft tissue in a joint because they are not changed during the inflammation process and do not strongly vary their positions. The 3D reconstructed images show distinct differences in their spatial distribution of the optical diffusion coefficient D for both cases. Clearly visible is the reduced volume occupied by the diffusion coefficient of the capsule in the rheumatoid stage (Fig. 5b).

We could observe that the reconstruction failed when using a high diffusion coefficient (e.g. $D=50\ cm^2 ns^{-1}$) assigned to the synovia. The reason for this kind of behavior is that our model is based on the diffusion equation, which is not able to describe the photon propagation very accurately in void-like tissue areas. In those cases transport theory based methods are required, which are a precise description of the photon migration in low scattering or low absorptive media like the synovial fluid of joints, the cerebrospinal fluid of the brain or the amniotic fluid of the female uterus.

5. SUMMARY

To overcome limiting assumptions of perturbation-theory-based reconstruction algorithms, we have developed a novel three-dimensional model-based reconstruction algorithm. We used this algorithm for reconstructing finger joints of healthy and rheumatoid conditions. We segmented MRI images and assigned known optical properties of different tissue types to get maps of the optical properties. Based on these maps we simulated measurement by calculating the detector readings with a time-dependent, finite-difference, diffusion forward model.

The reconstruction algorithm consists of three parts: 1) a finite difference based forward model of the time-dependent diffusion equation, 2) an image analysis scheme with an objective function and 3) a gradient calculation using adjoint differentiation. The gradient calculation is used to iteratively minimize the objective function with a line-minimization scheme. Starting from an initial guess we get, after several iterations, a reconstructed map of the optical properties.

The model based reconstruction method is able to reconstruct the healthy and the rheumatoid conditions of a finger joint. It can clearly be shown that changes of the diffusion coefficients of the capsule can be qualitatively and quantitatively reconstructed. Also we could observe that changes of the conditions of the synovial fluid can be monitored. Thus, optical tomography has the potential of becoming a novel imaging modality for rheumatoid diagnostics. Three-dimensional reconstructions show that the amount of voxels with diffusion coefficients lower than a defined threshold is decreased for the inflammated joint. This information gives an additional criterion for distinguishing healthy and rheumatoid conditions.

Our approach, which is based on the diffusion approximation, is currently not able to reconstruct areas with high diffusion coefficients because the diffusion theory does not reflect the physical reality in this case. Therefore, we suggest to use reconstruction algorithms based on the transport theory for void-like areas with little scattering.

6. REFERENCES

[1] K. Wells, J.C. Hebden. F.E.W. Schmidt, and D.T. Delpy, " The UCL multichannel time-resolved system for optical tomography", in Optical Tomograpgy and Spectroscopy of Tissue, B. Chance and R.R. Alfano, eds., Proceedings of the SPIE--The International society for Optical Engineering, vol. 2979, pp. 599-607 (1997).

[2] H. Jess, H. Erdl, K.T. Moesta, S. Fantini, M.A. Franceschini, E. Gratton, and M. Kaschke, "Intensity Modulated Breast Imaging: Technology and Clinical Pilot Study Results," in Advances in Optical Imaging and Photon Migration, OSA Trends in Optics and Photonics, Vol. II, R.R. Alfano and J.G. Fujimoto, eds., Optical Society of America, Washington, DC, pp. 126-129 (1996).

[3] J.P. Vanhouten, D.A. Benaron, S. Spilman, and D.K. Stevenson, "Imaging brain injury using time-resolved near-infrared light scanning," Pediatric Research 39, pp. 470-476 (1996).

[4] M. Miwa and Y. Ueda, "Development of time-resolved spectroscopy system for quantitative noninvasive tissue measurement," in Optical Tomography, Photon Migration, and Spectroscopy of Tissue and Model Media, B. Chance and R.R. Alfano, eds., Proceedings of the SPIE-The International Society for Optical Engineering, vol. 2389, pp.142-149 (1995).

[5] S. Fantini, M.A. Franceschini, J.S. Maier, S.A. Walker, B. Barbieri, and E. Gratton, "Frequency domain multichannel optical detector for noninvasive tissue spectroscopy and oximetry," Optical Engineering 34, pp.32-42 (1995).

[6] P.J. Kirkpatrick, "Use of near-infrared spectroscopy in the adult," Philosophical Transactions of the Royal Society of London - Series B: Biological Sciences 352, pp. 701-705 (1997).

[7] C. Hock, K. Villringer, F. Muller-Spahn, R. Wenzel, H. Heekeren, S. Schuh-Hofer, M. Hofmann, S. Minoshima, M. Schwaiger, U. Dirnagl, and A. Villringer, "Decrease in parietal cerebral hemoglobin oxygenation during performance of a verbal fluency task inpatients with Alzheimer's disease monitored by means of near-infrared spectroscopy (NIRS)--correlation with simultaneousr CBF-PET measurements," Brain Research 755, pp. 293-303 (xxxx).

[8] G. Buunk, J.G. van der Hoeven, and A.E. Meinders, "A comparison of near-infrared spectroscopy and jugular bulb oximetry incomatose patients resuscitated from a cardiac arrest," Anaesthesia 53, pp 13-19 (1998).

[9] L.C. Henson, C. Calalang, J.A. Temp, and D.S. Ward, "Accuracy of a cerebral oximeter in healthy volunteers under conditions ofisocapnic hypoxia," Anesthesiology 88, pp. 58-65 (1998).

[10] R.A. De Blasi, S. Fantini, M.A. Franceschini, M. Ferrari, and E. Gratton, "Cerebral and muscle oxygen saturation measurement by frequency-domainnear-infra-red spectrometer," Medical & Biological Engineering & Computing 33(2), pp. 228-30 (1995).

[11] W.J. Levin, S. Levin, and B. Chance, "Near-infrared measurement of cerebral oxygenation: correlation with electroencephalographic ischemia during ventricular fibrillation," Anesthesiology 83, pp. 738-746 (1995).

[12] T. Noriyuki, H. Ohdan, S. Yoshioka, Y. Miyata, T. Asahara, and K. Dohi, "Near-infrared spectroscopic method for assessing thetissue oxygenation state of living lung," American Journal of Respiratory & Critical Care Medicine 156, pp. 1656-1661 (1997).

[13] K.J. Sapire, S.P. Gopinath, G. Farhat, D.R. Thakar, A. Gabrielli, J.W. Jones, C.S. Robertson, and B. Chance, "Cerebral-oxygenation during warming after cardiopulmonary bypass," Critical Care Medicine 25, pp. 1655-1662 (1997).

[14] D.A. Benaron, J.P. Vanhouten, W. Cheong, E.L. Kermit, and R.A. King, "Ealry clinical results of time-of-flight optical tomography in a neonatal intensive care unit," Proceedings of the SPIE-The International Society for Optical Engineering, vol. 2389, pp. 582-596 (1995).

[15] W.F. Cheong, J.P. Vanhouten, E.L. Kermit, T.R. Machold, D.K. Stevenson and D.A. Benaron, "Pilot comparison of light-based optical tomography versus ultrasound for real-time imaging of neonatal intraventricular hemorrhage," Pediatric Research 39, pp. 1189 (1996).

[16] S.P. Gopinath, C.S. Robertson, C.F. Contant, R.K. Narayan, R.G. Grossman, and B. Chance, "Early detection of delayed traumatic intracranial hematomas using near-infrared spectroscopy," Journal of Neurosurgery 83, pp. 438-444 (1995).

[17] G. Gratton, M. Fabiani, P.M. Corballis, D.C. Hood, M.R. Goodman-Wood, J. Hirsch, K. Kim, D. Friedman, and E. Gratton, "Fast and localized event-related optical signals (EROS) in the human occipital cortex: comparisons with the visual evoked potential and fMRI," Neuroimage 6, pp. 168-80 (1997).

[18] A. Maki, Y. Yamashita, E. Watanabe, H. Koizumi, "Visualizing human motor activity by using non-invasive optical topography," Frontiers of Medical & Biological Engineering 7, pp. 285-97 (1996).

[19] C. Hirth, H. Obrig, J. Valdueza, U. Dirnagl, and A. Villringer, "Simultaneous assessment of cerebral oxygenation and hemodynamics during a motor task. A combined near infrared and transcranial Doppler sonography study," Advances in Experimental Medicine & Biology 411, pp. 461-469 (1997).

[20] A. Maki, Y. Yamashita, Y. Ito, E. Watanabe, Y. Mayanagi, and H. Koizumi, "Spatial and temporal analysis of human motor qactivity using noninvasive NIR topography," Medical Physics 22, pp. 1997-2005 (1995).

[21] R. Wenzel, H. Obrig, J. Ruben, K. Villringer, A. Thiel, J. Bernardinger, U. Dirnagl, And A. Villringer, "Cerebral blood oxygenation changes induced by visual stimulation in humans," Journal of Biomedical Optics 4, pp. 399-404 (1996).

[22] C. Hock, K. Villringer, F. Muller-Spahn, M. Hofmann, S. Schuh-Hofer, H. Heekeren, R. Wenzel, U. Dirnagl, and A. Villringer, "Near infrared spectroscopy in the diagnosis of Alzheimer's disease," Annals of the New York Academy of Sciences 777, pp. 22-29 (1996).

[23] A.J. Fallgatter, M. Roesler, L. Sitzmann, A. Heidrich, T.J. Mueller, and W.K. Strik, "Loss of functional hemispheric asymmetry in Alzheimer's dementia assessed with near-infrared spectroscopy," Brain Research, Cognitive Brain Research 6, pp. 67-72 (1997).

[24] O. Jarlman, R. Berg, S. Andersson-Engels, S. Svanberg, and H. Pettersson, "Time-resolved white light transillumination foroptical imaging," Acta Radiologica 38, pp. 185-189 (1997).

[25] S. Nioka, Y. Yung, M. Shnall, S. Zhao, S. Orel, C. Xie, B. Chance, and L. Solin, "Optical imaging of breast tumor by means of continuous waves," Advances in Experimental Medicine & Biology 411, pp. 227-32 (1997).

[26] B.J. Tromberg, O. Coquoz, J.B. Fishkin, T. Pham, E.R. Anderson, J. Butler, M. Cahn, J.D. Gross, V. Venugopalan, D. Pham, "Non-invasive measurements of breast tissue optical properties using frequency-domain photon migration," Philosophical Transactions of the Royal Society of London - Series B: Biological Sciences, 352, pp. 661-668 (1997).

[27] R.R. Alfano, S.G. Demos, and S.K. Gayen, "Advances in optical imaging of biomedical media," Annals of the New York Academy of Sciences 820, pp. 248-70; Discussion 271 (1997).

[28] M.A. Franceschini, K.T. Moesta, S. Fantini, G. Gaida, E. Gratton, H. Jess, W.W. Mantulin, M. Seeber, P.M. Schlag, and M. Kaschke, "Frequency-domain techniques enhance optical mammography: initial clinical results," Proceedings of theNational Academy of Sciences of the United States of America 94, pp. 6468-6473 (1997).
[29] S. Fantini, M.A. Franceschini, G. Gaida, E. Gratton, H. Jess, W.W. Mantulin, K.T. Moesta, P.M. Schlag, and M. Kaschke, "Frequency-domain optical mammography: edge effect corrections," Medical Physics 23(1), pp. 149-57 (1996).
[30] V.Prapavat,R.Schuetz,W.Runge,J.Beuthan,G.Mueller, "In-Vivo-investigations on the detection of chronical polyarthritis using a cw-transillumination method at interphalangeal joints", SPIE Vol. 2626, pp. 360-366 (1995).
[31]J.Beuthan, R.Freyer, O.Minet, C.Tran Luu, U.Hampel, R.-D.Naber, G.Müller,"Optical Tomography of a rat brain", SPIE Vol.2676, 1995.
[32] A.Klose, V.Prapavat, O.Minet, J.Beuthan, G.Mueller, "RA diagnostics applying optical tomography in frequency-domain", in SPIE Proceedings 3196, pp.194-204, 1997.
[33] S. B. Colak, D. G. Papaioannou, G. W. 't Hooft, M. B. van der Mark, H. Schomberg, J. C. J. Paasschens, J. B. M. Melissen, and N. A. A. J. van Asten, "Tomographic image reconstruction from optical projections in light-diffusing media," Appl. Opt. 36, pp. 180-213 (1997).
[34] S.A. Walker, S. Fantini, and E. Gratton, "Image recon-struction by backprojection from frequency domain optical measurements in highly scattering media," Appl. Opt. 36, pp. 170-179 (1997).
[35] R. L. Barbour, H. L. Graber, J. W. Chang, S. L. S. Barbour, P. C. Koo, R. Aronson, "MRI-guided optical tomography: Prospects and computation for a new imaging method," IEEE Computational Science & Engineering 2, 63-77 (1995).
[36] M. A. Oleary, D. A. Boas, A. G. Yodh, "Experimental images of heterogeneous turbid media by frequency-domain diffusing photon tomography," Opt. Lett. 20, pp. 426-428 (1995).
[37] Y. Q. Yao, Y. Wang, Y. L. Pei, W. W. Zhu, R. L. Barbour, " Frequency-domain optical imaging of absorption and scattering distrinbutions by Born iterative method," J. Opt. Soc. Am. A 14, pp. 325-342 (1997).
[38] M. Schweiger and S.R. Arridge, " A system for solving the forward and Inverse Problems in optical spectroscopy and imaging," in Advances in Optical Imaging and Photon Migrations, OSA Trends in Optics and Photonics Series, vol. 2, R.R. Alfano and J.G. Fujimoto, eds., Optical Society of America, Washington, DC, 1996
[39] H. B. Jiang, K. D. Paulsen, U. L. Osterberg, B. W. Pogue, and M. S. Patterson, "Optical image recon-struction using frequency domain data: Simulations and experiments," J. Opt. Soc. Am. A 13, pp. 253-266 (1996).
[40] A.H. Hielscher, "Model-Based Iterative Image Reconstruction for Photon Migration Tomography," in Methods for Solving Ill-Posed Inverse Imaging Problems: Medical and Nonmedical Applications, R.L. Barbour, M.J. Carvlin, and M.A. Fiddy, eds., SPIE-The International Society of Optical Engineering , Proc. 3171, pp.106-117, (1997).
[41] A.H. Hielscher, A. Klose, D.M. CatariousJr., K.M. Hanson, "Tomographic imaging of biological tissue by time-resolved, model-based, iterative, image reconstruction," in OSA Trends in Optics and Photonics on Advances in Optical Imaging and Photon Migration II, J.G. Fujimoto, M. Patterson, R.R. Alfano, eds., Optical Society of America, Washington, DC 1998. (in press)
[42] R.C.Lawrence, C.G.Helmick, F.C.Arnett, R.A.Deyo, "Estimates of the prevalence of arthritis and selected musculoscetal disorders in the United States", Arthritis&Rheumatism 41, 778-799, 1998
[43] J.T.Sharp,"Assessment of radiographic abnormalities in rheumatoid arthritis : What have we accomplished and where should we go from here?",J.Rheumatol 22,1787-1791 (1995)
[44] M. Ostergaard, M. Stoltenberg, P. Lovgreen-Nielsen, B. Volck, C.H. Jensen, I.B. Lorenzen, "Magnetic resonance imaging determined synovial membrane and joint effusion volumes in rheumatoid arthritis and osteoarthritis," Arthritis & Rheumatism 40, pp. 1856-1867 (1997).
[45] A.Lehtinnen,L.Paimela, J.Kreula, M.Leirisalo-Repro,"Painful ankle region in rheumatoid arthritis - Analysis of soft-tissue changes with ultrasonography and MR imaging", Acta Radiologica 37, pp. 572-577, (1996).
[46] V.Prapavat: "Anwendung der experimentellen Systemanalyse zur Informationsgewinnung aus Streulicht im Frühstadium entzündlich-rheumatischer Veränderungen"; PhD thesis; Technical University Berlin; 1997.
[47] V. Prapavat, W. Runge, J. Mans, A. Krause, J. Beuthan, and G.Muller ,"The development of a finger joint phantom for the optical simulation of early inflammatory rheumatic changes," (German) Biomedizinische Technik , vol. 42, pp. 319-326, 1997.
[48] W.F. Ames, Numerical Methods for Partial Differential Equations, Academic Press, New York, NY, 1977, pp. 148-157.
[49] W.H. Press, S. A. Teukolsky, W.T. Vetterling, and B.P. Flannery, Numerical Recipes in C, Cambridge University Press, New York, NY, 1992.
[50] S. S. Saquib, K. M. Hanson, and G. S. Cunningham, "Model-based image reconstruction from time-resolved diffusion data", in Medical Imaging: Image Processing, Proc. of the SPIE-The International Society for Optical Engineering, vol. 3034, pp. 369-380, 1997.
[51] D.W.Stoller,"Magnetic Resonance Imaging in Orthopaedics and Sports Medicine", Lippincott-Raven, New York, 2nd edition, 1997